Investigation of the magnetocaloric effect in double distorted perovskites $Ca(Cu_{3-x}Mn_x)Mn_4O_{12}$ ($1 \leqslant x \leqslant 2$): From standard ferrimagnetism to glassy ferrimagnetism

Q. Zhang,* Y. Bréard, F. Guillou, and V. Hardy

Laboratoire CRISMAT, UMR 6508, CNRS ENSICAEN, 6 Boulevard du Maréchal Juin, F-14052 Caen Cedex 4, France

(Received 22 August 2011; revised manuscript received 15 October 2011; published 27 December 2011)

The double-distorted perovskites $Ca(Cu_{3-x}Mn_x)Mn_4O_{12}$ ($x = 1$, 1.25, 1.5, and 2) exhibit a paramagnetic-to-ferrimagnetic transition at a temperature decreasing from $T_C \approx 280$ K for $x = 1$ down to $T_C \approx 163$ K for $x = 2$. In the latter compound a re-entrantlike spin-glass state emerges around $T_g \approx 70$ K. For each composition the isothermal entropy change ΔS_M was derived from magnetic measurements recorded up to 9 T. The obtained $\Delta S_M(T)$ curves exhibit a broad and dissymmetric distribution, leading to high values of refrigerant capacity. The impact of the x value on the magnetic and magnetocaloric properties is addressed in detail, taking into account the various spin interactions present in these compounds.

DOI: 10.1103/PhysRevB.84.224430 PACS number(s): 75.30.Sg, 75.50.Lk, 75.50.Gg, 75.30.Cr

I. INTRODUCTION

Magnetic refrigeration is a technology based on the magnetocaloric effect (MCE) that is expected to become competitive with traditional gas-compression cooling methods since it has a potentially higher energy efficiency while being environmentally friendly.[1] In the last decade many efforts have been made to explore magnetocaloric materials exhibiting large values of the isothermal entropy changes $-\Delta S_M$. The greatest attention is generally paid to the maximum value, $-\Delta S_M^{\max}$, that is found near the magnetic transition temperature. However, the refrigerant capacity (RC), which does not depend only on the maximum but rather on the overall profile of $-\Delta S_M(T)$, is probably a more relevant parameter to characterize the effectiveness of a material for refrigeration applications.[2–4]

The giant $-\Delta S_M^{\max}$ values around room temperature (RT) reported in the last years have always been observed in materials showing a first-order magnetic transition (FOMT), such as $Gd_5(Ge_{1-x}Si_x)_4$,[5] $MnAs_{1-x}Sb_x$,[6] $LaFe_{13-x}Si_x$,[7] and $MnFeP_{0.45}As_{0.55}$,[8] etc.[9] It must be realized, however, that the quite narrow working temperature region often associated to such FOMTs is a drawback which can limit their application. Moreover, the presence of thermal and magnetic hysteresis can considerably reduce the actual RC of these materials.[3] Last but not least, slow kinetics[4] and premature ageing[9] that can be caused by the magneto-structural nature of these transitions are other phenomena that can be detrimental to applications in refrigerating cycles.

Compared to materials undergoing a FOMT, those showing a second-order magnetic transition (SOMT) usually possess a lower $-\Delta S_M^{\max}$, but they can have a comparable or even larger RC, and they do not suffer from the aforementioned drawbacks. Therefore, the magnetic materials with a SOMT must still be regarded as interesting candidates for the development of magnetic refrigeration devices.[10] In particular, one observes that Gadolinium remains the most studied material for RT magnetic refrigeration, in spite of its quite high cost. In this context the exploration of new, cheap magnetocaloric materials based on SOMT and showing a large RC is still a topical issue.

The $AA'_3Mn_4O_{12}$ family[11–14] (where A can be monovalent, divalent, or trivalent while A′ is Cu^{2+} or Mn^{3+}) is also known as the double-distorted perovskitelike structure. This particular structure is stabilized owing to the Jahn-Teller nature of the A′ cations, which distorts the usual cubo-octahedral sites of the perovskite to a nearly square oxygen environment. It turns out that the presence of magnetic cations (Cu^{2+} or Mn^{3+}) on these sites can yield magnetization values that are larger than in standard "single" perovskite manganites, a feature which would be of interest in terms of MCE.

One prototypical example of this family, $CaCu_3Mn_4O_{12}$, whose cation distribution is $Ca^{2+}Cu_3^{2+}Mn_4^{4+}O_{12}$, exhibits a ferrimagnetic (FI) transition above RT ($T_C = 355$ K),[11,15] with a saturation magnetization (M_S) of $\sim 9\mu_B$/f.u.[16,17] It is known that Cu^{2+} ions can be partially or completely substituted by Mn^{3+} on the A′ site, giving rise to compositions $Ca(Cu_{3-x}Mn_x)Mn_4O_{12}$.[18,19] Such aliovalent substitution on the A′ sites is counterbalanced by a formal charge transfer from Mn^{4+} to Mn^{3+} on the B sites, leading to a cation distribution, which can be written as $Ca^{2+}(Cu_{3-x}^{2+}Mn_x^{3+})_{A'}(Mn_{4-x}^{4+}Mn_x^{3+})_BO_{12}$.[19,20]

Previous results of the literature[13,21–23] have shown that these substituted compounds can increase M_S while decreasing T_C toward RT. Both these features can be beneficial regarding the MCE at RT. Moreover, it was also reported about the presence of competing exchange interactions[13] among the numerous magnetic species that are in play. Such a situation can lead to complex magnetic states, for which the MCE was not yet investigated. Motivated by these issues, we synthesized the $Ca(Cu_{3-x}Mn_x)Mn_4O_{12}$ compounds with four x values within the interval $1 \leqslant x \leqslant 2$ and studied the effects of this substitution content on the magnetic and magnetocaloric properties.

II. EXPERIMENTAL DETAILS

Polycrystalline $Ca(Cu_{3-x}Mn_x)Mn_4O_{12}$ ($x = 1$, 1.25, 1.5, and 2) compounds were prepared using a method similar to that of Ref. 19 but under a lower pressure of 110 bar. Stoichiometric amounts of high-purity $CaCO_3$, CuO, and $Mn(NO_3)_2$ powders are dissolved in an excess amount of nitric acid. During the dissolution process, citric acid and ethylene glycol are also added. Then, ethylenediamine is added until the solution becomes basic, as tested by litmus paper. The solution is then slowly evaporated, and a black powder is obtained after the

organic components are decomposed at 600 °C. In a next step this black powder is pressed into pellets and sintered under an oxygen pressure of 110 bar for 60 h at a "preparation" temperature T_p (being either 900 °C or 700 °C) with one intermediate grinding. As will be discussed subsequently, increasing T_p tends to increase M_S, which is the main reason why we focused on the series prepared at 900 °C in the present work.

The structural characterization has been carried out by means of a Panalytical Xpert Pro diffractometer using Cu-K_α radiations. The structural Rietveld refinements were performed using FULLPROF program incorporated in the WinPLOTR Package. Selected area electron diffraction (SAED) was performed on a JEOL 2010 microscope equipped with an ultra low-temperature double-tilt helium-cooling holder (ULTDT Gatan). Investigations were performed from RT down to the lowest reachable temperature, which is estimated to be around 20 K.[24–26] The *dc* temperature/field dependence of magnetization and the frequency dependence of the *ac* susceptibility were recorded by means of an extraction technique in a Physical Properties Measurement System (PPMS, Quantum design).

III. RESULTS AND DISCUSSION

A. Structural characterization

In $AA'_3B_4O_{12}$, the crystal symmetry exhibits a doubling of the ideal ABO_3 perovskite cell due to the ordering of the A and A′ ions and the associated distortion of the oxygen sublattice, which results in a tilted three-dimensional network of BO_6 octahedra-sharing corners (Fig. 1). The cations Cu^{2+} and Mn^{3+} in position A′ locate in square environment of O^{2-} ions, whereas the cations in position B lie in octahedral environment of O^{2-} ions.

All the structures of the series $Ca(Cu_{3-x}Mn_x)Mn_4O_{12}$ (x = 1, 1.25, 1.5, and 2) prepared at 900 °C can be well refined in the aristotype $Im\bar{3}$ space group with $a = 2a_p$ unit-cell parameter (a_p is a unit cell of the perovskite aristotype), confirming that our samples crystallize with the expected-ordered perovskite

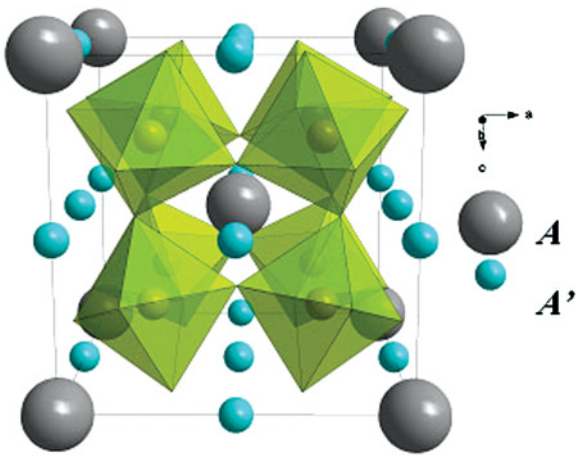

FIG. 1. (Color online) A view of the crystallographic structure of $AA'_3B_4O_{12}$. Large and small spheres represent A and A′ cations, respectively. The cations B are located inside the octahedra.

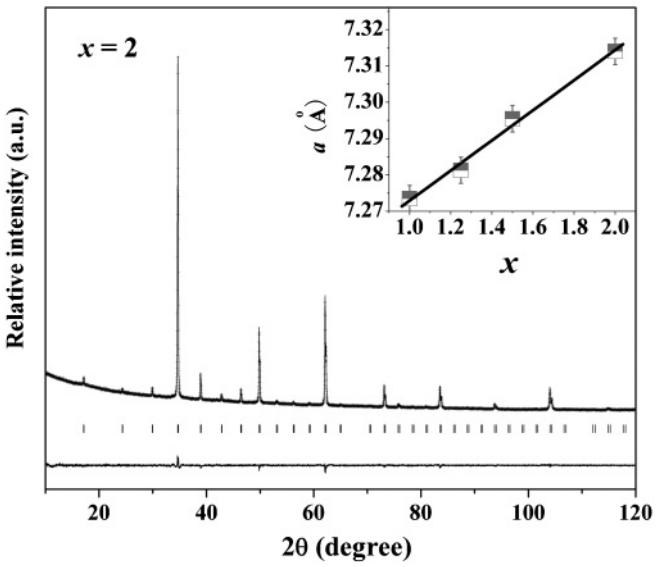

FIG. 2. Observed (+), calculated (solid line), and difference (below) x-ray diffraction pattern for $Ca(CuMn_2)Mn_4O_{12}$ determined at RT. The marks indicate the allowed reflexions in the space group $Im\bar{3}$. Insert: evolution of the cell parameter a as a function of x in $Ca(Cu_{3-x}Mn_x)Mn_4O_{12}$.

phase. An example of a refined single-phase x-ray diffraction pattern for $x = 2$ sample is given in Fig. 2. Moreover, it was found that the cell parameter a exhibits a linear evolution with x (see insert of Fig. 2), a behavior consistent with the larger ionic radii of Mn^{3+} (0.78 Å) compared to Cu^{2+} (0.71 Å) and Mn^{4+} (0.67 Å).[23] This result is in good agreement with previous works[27] and confirms the random substitution of Cu^{2+}/Mn^{3+} on the A′ sites.[20]

For the compounds with $A' = Cu^{2+}$, it is known that there is no charge separation Mn^{3+}/Mn^{4+} on the B sites, whereas those for which $A' = Mn^{3+}$ always lead to a phenomenon of charge and orbital ordering within the B sublattice as the temperature is decreased.[13,28] To investigate this issue in the present case of mixed Cu^{2+}/Mn^{3+} occupancy on the A′ sites, we performed SAED versus temperature on our highest substitution content ($x = 2$). Down to our lowest temperature (∼20 K), the reconstructions of the reciprocal space show that the system of reflections is still consistent with the $Im\bar{3}$ space group (see Fig. 3), demonstrating the absence of any distortion marking the setting of cooperative Jahn-Teller effect. This result clearly states that even with ($x = 2$) (which is *a priori* situation expected to be the most favorable to charge ordering since the average valence is 3.5+), the Mn charges on the B site remain disordered.

This absence of Mn^{3+}/Mn^{4+} ordering is consistent with the results of XANES experiments performed by Sánchez-Benítes *et al.*[20] on the same series of $Ca(Cu_{3-x}Mn_x)Mn_4O_{12}$ materials for $x = 0.55$, 1, and 2. Beyond the absence of charge ordering, it was even shown that one cannot distinguish the spectroscopic signatures of pure Mn^{3+} and Mn^{4+}, which indicates that—at least down to the temperature investigated in this study, i.e., 40 K—one should just consider that Mn has an *intermediate* valency equal to $4 - x/4$.

The $Ca(Cu_{3-x}Mn_x)Mn_4O_{12}$ series prepared under 700 °C also showed the formation of the expected phase, but with a

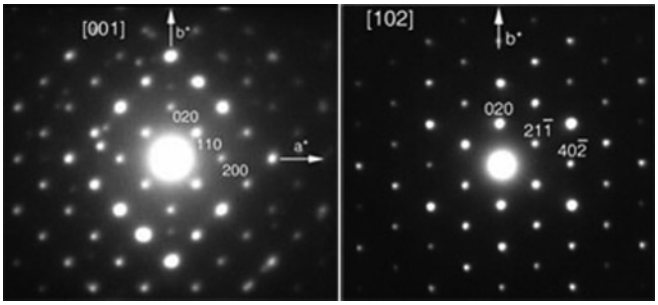

FIG. 3. [001] and [102] SAED patterns of $Ca(CuMn_2)Mn_4O_{12}$ recorded at our lowest temperature (≈20 K). These patterns are typical of the space group $Im\bar{3}$, without any additional superstructure spots as it would be expected in case of charge ordering.

small amount of Mn_2O_3 as a secondary phase (mass content less than 5%), another reason why we focused on the 900 °C series.

B. Role of x in the magnetic transitions

Figure 4 displays zero-field-cooled (ZFC) and field-cooled (FC) magnetization curves, recorded in a small magnetic field of 0.01 T, for the whole series of $Ca(Cu_{3-x}Mn_x)Mn_4O_{12}$. When decreasing the temperature, a sharp increase in magnetization takes place at high temperature for all the compounds, due to the paramagnetic (PM)-FI transition. The corresponding T_C, defined as the temperature of the peak in the first derivative of the ZFC curve, decreases from 280 K to 163 K when x is increased from 1 to 2. In the compounds with $x = 1$, 1.25, and 1.5, one observes a roughly constant shift between the

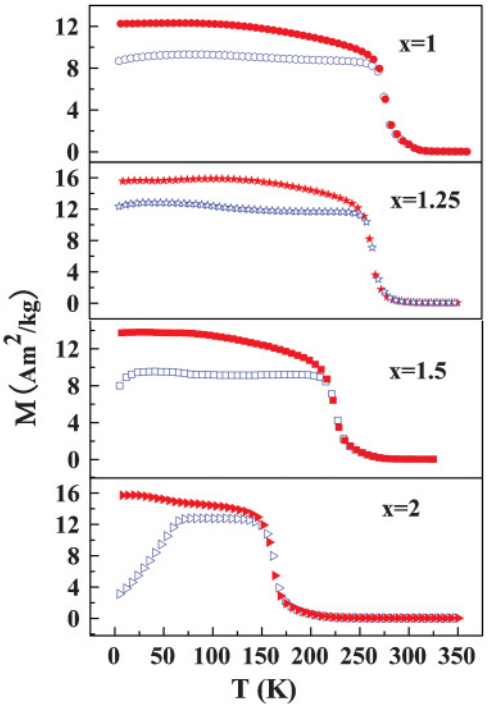

FIG. 4. (Color online) Temperature dependences of the ZFC (open symbols) and FC (solid symbols) magnetization in 0.01 T, recorded in the $Ca(Cu_{3-x}Mn_x)Mn_4O_{12}$ compounds with $x = 1$, 1.25, 1.5, and 2.

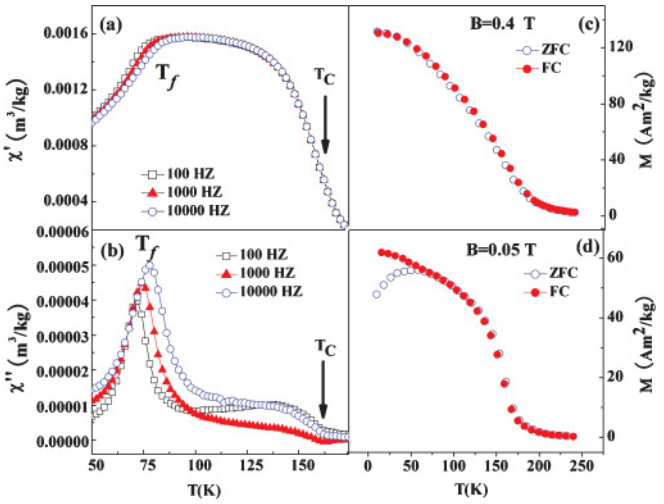

FIG. 5. (Color online) Magnetic measurements recorded in $Ca(CuMn_2)Mn_4O_{12}$ (i.e., the $x = 2$ compound): Temperature dependences of (a) the in-phase (χ') and (b) out-of-phase (χ'') *ac* susceptibility measured at different frequencies; temperature dependences of the ZFC and FC magnetization measured in a *dc* field equal (c) 0.4 T and (d) 0.05 T.

ZFC and FC curves, which rises just below T_C. We performed *ac* susceptibility measurements, which showed the absence of any frequency dependence around this bifurcation between the ZFC and FC curves, indicating that this feature does not mark the onset of a glassy behavior. Instead, such a small difference between ZFC/FC curves in a low field like 0.01 T may be ascribed to an effect of domain-wall pinning, leading to a larger magnetization upon field cooling.[29]

The situation is different for $x = 2$, i.e., the $CaCuMn_6O_{12}$ compound. Below about 75 K, the ZFC magnetization decreases rapidly, while the FC curve keeps increasing. On the basis of this shape of the ZFC curve, Vasil'ev *et al.*[30] first proposed the onset of a spin-glass (SG) state in $CaCuMn_6O_{12}$. To further support this idea, we investigated the frequency dependence of χ_{ac} in this compound, between 10^2 and 10^4 Hz. As shown in Figs. 5(a) and 5(b), the in-phase χ' exhibits frequency dependence in a temperature range located just below 75 K, which can be regarded as a first clue supporting a SG behavior. Focusing on the out-of-phase χ'', which yields well-defined peaks, one observes that increasing the frequency not only induces a shift toward higher temperatures but also an increase in intensity. It turns out that it is exactly the overall behavior expected for a SG transition.[31,32] Ascribing the characteristic freezing temperature T_f to the location of the peak in $\chi''(T)$, one can quantify the phenomenological parameter $p = (\Delta T_f/T_f)/\Delta \log f$. One obtains a value $p \approx 0.042$, which is well within the range (0.004–0.080) typical of SG materials.[31] Finally, one can remark that T_f at our lowest frequency (100 Hz) is well consistent with the kink found on the ZFC curve in a very low *dc* field (0.01 T), providing us with an estimate of the underlying glass transition close to $T_g \approx 70$ K.

The glassy features of $CaCuMn_6O_{12}$ were addressed only a few times in the literature. While Volkova *et al.*[33] ascribed the frustration to antagonist couplings within the $(Mn^{3+})_{A'}$-$(Mn)_B$ superexchange (SE) interaction, Zhang *et al.*[34] rather

suggested that the frustration lies within the $(Mn)_B$ sublattice itself and gives rise to a cluster-glass (CG). In other respects, since a long-range FI ordering exists at a higher temperature ($T_C \approx 163$ K), we suggest this SG may also be regarded as a re-entrant spin glass (RSG).[35–37] The *dc* magnetization was measured from 5 to 240 K in different magnetic fields [shown in Figs. 5(c) and 5(d). In a field as low as 0.05 T, the signatures of SG are already much weakened, but one can still detect a broad peak on the ZFC curve, as well as a bifurcation between ZFC and FC in the low-T range. However, as soon as the field reaches 0.4 T, the ZFC and FC becomes well superimposed on each other and all indications of a SG behavior have totally disappeared. Such a rapid vanishing of the "glassiness" when the field is increased is qualitatively consistent with a RSG.[36,37] The fact remains that, even within such a framework, the details of the mechanisms at the origin of a glassy behavior in $CaCuMn_6O_{12}$ are still unclear.

It is well known that the two basic ingredients required to yield any SG behavior are the presence of (i) randomness and (ii) antagonist interactions.[31] While the first feature is indeed expected owing to the random distribution of Cu^{2+}/Mn^{3+} on the A′ sites, the nature of the competing interactions leading to frustration is much more controversial.[33,34] In what follows we present a still different picture putting into play the coupling among the $(Mn^{3+})_{A'}$ themselves.

In $CaCu_3Mn_4O_{12}$, it was first shown by Weht *et al.*[17] that the transition at 355 K is a FI ordering resulting from a strong antiferromagnetic (AF) coupling between the Cu^{2+} moments in position A′ and the Mn^{4+} moments in position B. This strong AF coupling is present independently of the average valence of $(Mn)_B$, as demonstrated by the magnetic properties of $ThCu_3Mn_4O_{12}$, for which the formal valence of $(Mn)_B$ is 3.5, i.e., equal to that of $x = 2$ in the present study.[38] In the series $Ca(Cu_{3-x}Mn_x)Mn_4O_{12}$, one can thus assume that the AF coupling $(Cu^{2+})_{A'}$-$(Mn)_B$ remains the leading interaction over the investigated x range ($\leqslant 2$). Note that the situation is very different in materials with only Mn on the A′ sites, i.e., the series AMn_7O_{12} (with A being either monovalent, divalent or trivalent), for which it was found that the interaction between $(Mn^{3+})_{A'}$ and $(Mn)_B$ is very weak, whatever the average valence of $(Mn)_B$ is.[13,28] On the other hand, there is a substantial AF interaction among the $(Mn^{3+})_{A'}$ in the AMn_7O_{12} compounds, which can even yield long-range magnetic ordering at quite high temperatures within this A′ sublattice.[13,28]

When Mn^{3+} substitutes for Cu^{2+} on the A′ sites, different modifications must be taken into account. First, the dominant AF-SE interaction between the A′ and B sublattices is reduced, an effect which well accounts for the fast decrease observed in T_C. Second, this substitution decreases the average Mn valence on the B sites, which thus departs from the pure Mn^{4+} scheme existing for $x = 0$. Such a mixed Mn valency on the B sites, in addition to the presence of two types of cations on the A′ sites, gives rise to a great variety of magnetic interactions. Moreover, it is difficult to anticipate the nature of most of these couplings, since the Mn-O-Mn angles involved in the SE are ∼140° for B-O-B and ∼110° for A′-O-B,[12,33] i.e., well shifted from the best documented cases (180° and 90°) and not far from the crossover angle where the interactions change their sign.[39,40] However, taking into account the absence of charge ordering between Mn^{3+} and Mn^{4+} on the B sites, one can consider that the average SE coupling within this sublattice should be globally AF (as for 180°) but weak, while a ferromagnetic (FM) double-exchange mechanism must come into play.[33,39,41,42] About $(Mn^{3+})_{A'}$-$(Mn)_B$, one also expects antagonist SE interactions, but still weaker, in such a way that the resulting overall interaction must be very small.[33] Recently, results of neutron diffraction on $La(Cu_{3-x}Mn_x)Mn_4O_{12}$ led Muñoz *et al.*[43] to suggest a weak FM coupling for $(Mn^{3+})_{A'}$-$(Mn)_B$. Finally, three types of interactions must be considered within the A′ sites: $(Cu^{2+})_{A'}$-$(Cu^{2+})_{A'}$, $(Cu^{2+})_{A'}$-$(Mn^{3+})_{A'}$, and $(Mn^{3+})_{A'}$-$(Mn^{3+})_{A'}$: (i) In our compounds with magnetic 3*d* cations on the B sites, $(Cu^{2+})_{A'}$-$(Cu^{2+})_{A'}$ is more likely FM;[44] (ii) the case of $(Cu^{2+})_{A'}$-$(Mn^{3+})_{A'}$ is still under debate, even though a few papers claimed an AF coupling;[38,42] (iii) as for $(Mn^{3+})_{A'}$-$(Mn^{3+})_{A'}$, it is widely admitted that this coupling is strongly AF.[13]

In this survey of the interactions, one can recognize the first two suggestions made to interpret the SG in $x = 2$, i.e., a spin frustration involving either $(Mn)_B$-$(Mn)_B$[34] or $(Mn^{3+})_{A'}$-$(Mn)_B$.[33] It turns out, however, that a third mechanism naturally emerges from the previous picture. Indeed, one can consider that the $(Mn^{3+})_{A'}$ are subject to spin frustration in the sense that their "internal" interaction favors an antiparallel alignment, whereas their interactions with $(Cu^{2+})_{A'}$ and $(Mn)_B$—whatever their signs—tend to polarize them in a FM-like fashion. Since these $(Mn^{3+})_{A'}$ are spatially disordered over the A′ sublattice, they are thus submitted to random and antagonist interactions, i.e., a situation which must lead to a SG behavior.

C. Role of x in the saturation magnetization

Figure 6 indicates that the $Ca(Cu_{3-x}Mn_x)Mn_4O_{12}$ compounds exhibit large magnetization values which increase with the Mn/Cu ratio. For all x values, the $M(B)$ loops at 5 K show a soft magnetic character, without substantial hysteresis. For the lowest x values (1, 1.25, and 1.5), the magnetization is found to be saturated at quite low fields of the order of ∼0.5 T. The only exception is $x = 2$ for which the magnetization is not saturated

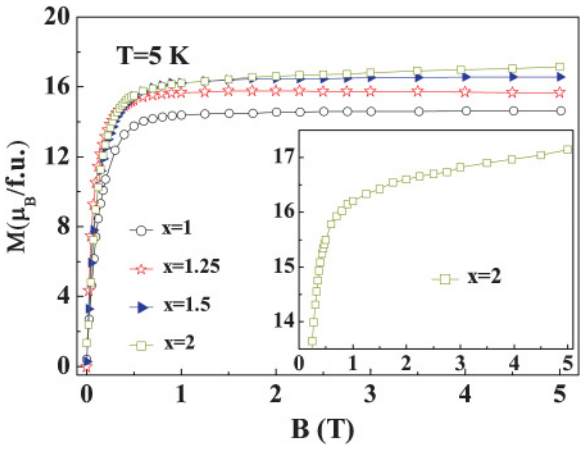

FIG. 6. (Color online) Magnetization curve recorded at 5 K in the compounds of the series $Ca(Cu_{3-x}Mn_x)Mn_4O_{12}$. The inset is an enlargement of the $x = 2$ curve, exhibiting the absence of saturation trend up to 5 T for this composition.

even at 5 T (see inset of Fig. 6). Actually, a closer look at the data indicates that the magnetization first exhibits a rapid rise with B as for the lower x values, but then it keeps increasing with a much smaller slope, showing no sign of saturation up to 5 T. A previous study by Volkova *et al.* using pulsed field,[33] demonstrated that magnetization only shows a trend to saturation towards $\sim$20 μ_B/f.u. when approaching 45 T. In the present study a value of $\sim$17.1 μ_B/f.u. is obtained in 5 T, which is a bit larger than that in the previous reports. We suggest this difference might be ascribed to the preparation temperature T_p, which is higher (900 °C) than those used previously.[11,19] This tendency is confirmed in our own data by the evolution of M_S for $x = 1.25$ that increases from 14.4 to 15.7μ_B/f.u. when T_p is increased from 700° to 900° [see Fig. 7]. Moreover, all the compositions show that a higher T_p induces a decrease in T_C (see Fig. 7), a feature which can account for the fact that our Curie temperatures are a bit lower than those reported by Zeng *et al.*[19] In a detailed investigation of the $x = 2$ compound, Itkis *et al.*[27] interpreted such a decrease in T_C as T_p is increased by the appearance of a small amount of antisite defects resulting in partial occupation of octahedral B sites by Cu^{2+}.

The evolution of M_S versus x in $Ca(Cu_{3-x}Mn_x)Mn_4O_{12}$ is reported in Fig. 7. While the M(5 K; 5 T) well reflects M_S for $x < 2$, we had to use the result of Ref. 33 for $x = 2$. It must be specified that one refers here to the "saturation magnetization" of the FI state, i.e., a configuration where the spins of $(Cu^{2+})_{A'}$ and $(Mn)_B$ remain antiparallel to each other. Indeed, the AF $(Cu^{2+})_{A'}$-$(Mn)_B$ coupling is too large to be broken by any magnetic field up to at least 45 T.[33] To discuss the expected variation of $M_S(x)$, let us consider the formal expression $Ca^{2+}[(Cu^{2+}_{3-x}Mn^{3+}_x)]_{A'}(Mn^{4+}_{4-x}Mn^{3+}_x)_B O_{12}$. For all present magnetic cations, one can safely assume a Landé factor equal to 2 and the following spin values: $Cu^{2+}(S = 1/2)$, $Mn^{3+}(S = 2)$, and Mn^{4+} $(S = 3/2)$. It is clear that substituting Mn for Cu leads to increase the magnetization on both the A′ and B sublattice, but two cases should be distinguished: if the spins of all cations on A′ are antiparallel to those of Mn on

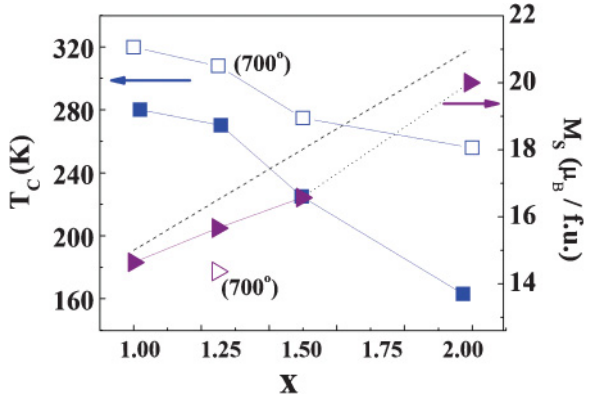

FIG. 7. (Color online) Variation of the FI transition temperature (T_C; filled squares) and of the saturation magnetization (M_S; filled triangles) as a function of x in the $Ca(Cu_{3-x}Mn_x)Mn_4O_{12}$ series prepared at $T_p = 900$ °C. The dashed line is the calculated $M_S = (9 + 6x)\ \mu_B$/f.u. The M_S of $x = 2$ was taken from Ref. 33 (connected by the dotted line to our experimental data at lower x). The open square symbols correspond to the T_C in the $Ca(Cu_{3-x}Mn_x)Mn_4O_{12}$ series prepared at $T_p = 700°$. The open triangle shows the M_S of $x = 1.25$ prepared at $T_p = 700°$.

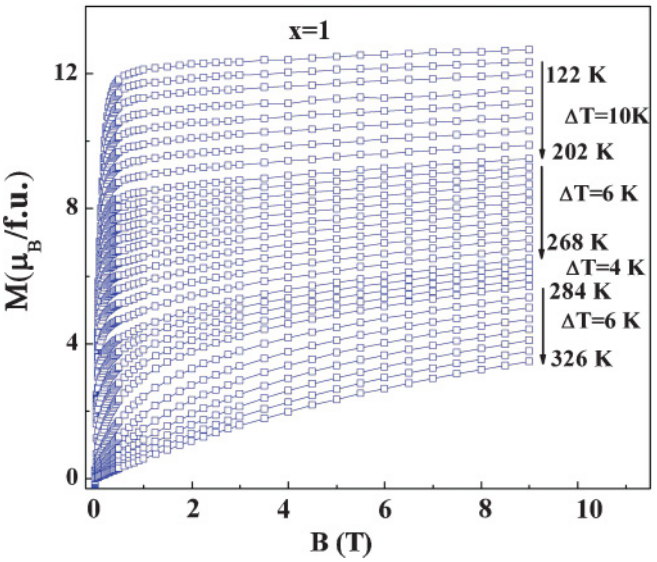

FIG. 8. (Color online) Series of magnetic isotherms recorded in the $x = 1$ compound.

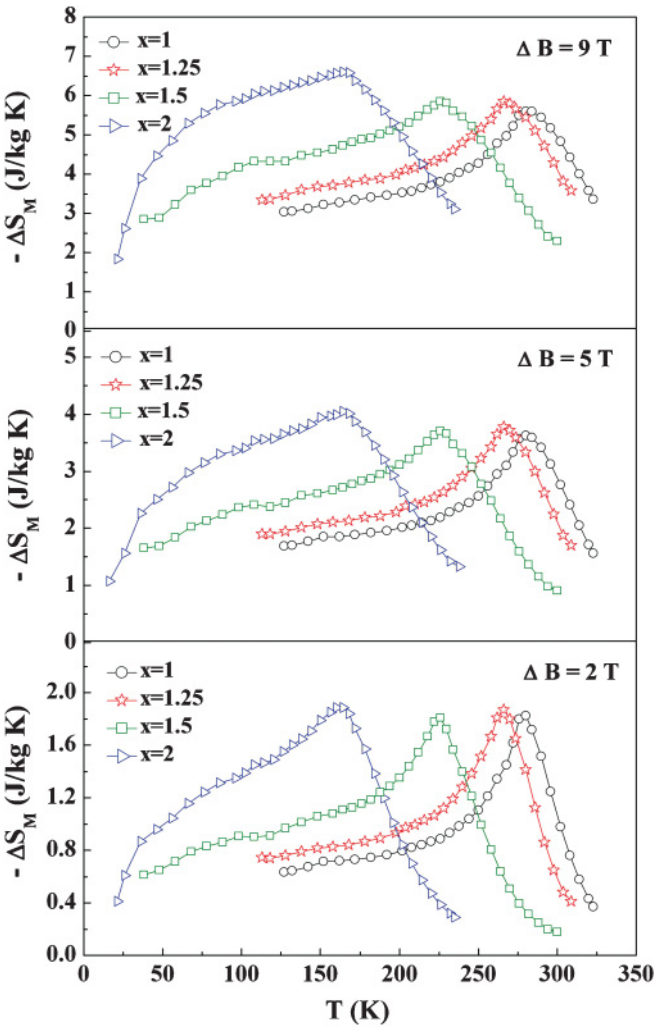

FIG. 9. (Color online) Temperature dependence of the isothermal entropy change in $Ca(Cu_{3-x}Mn_x)Mn_4O_{12}$ ($x = 1$, 1.25, 1.5, and 2) compounds for field changes equal to 2 T, 5 T, or 9 T.

B, the expected M_S is $(9-2x)\mu_B$/f.u., whereas if only the spins of Cu^{2+} remain antiparallely oriented, one has $M_S = (9+6x)\mu_B$/f.u. The experimental data of Fig. 7 clearly shows that the former hypothesis can be discarded, while reasonable consistency is found with the latter. Note, however, that the observed M_S are systematically lower than those calculated within the frame of the simple model described previously. Actually, spin configurations derived from neutron analysis pointed to a more complex arrangement involving some canting at the A′ sites.[21,38] In the most recent investigation, it was reported that the magnetic moment of $(Mn^{3+})_{A'}$ for $x = 0.5$ remains oriented at an angle of 96° with respect to that of $(Cu^{2+})_{A'}$ even in large fields (instead of being 180° as in the previous scenario).[21] Such a canting effect could explain that the observed M_S are slightly smaller than the expected values.

Turning back to the SG behavior found in $x = 2$, it must be emphasized that the observed M(B) curve is very different from the S-shape expected for conventional SG.[31] Rather, there is firstly a rapid polarization ($B \leqslant 1$ T) to $\sim 16\mu_B$/f.u. that is followed by a continuous increase, reaching $\sim 17.1\mu_B$/f.u. in 5 T (actually, this behavior extends up to much larger magnetic fields to reach about $20\mu_B$/f.u.).[33] Note that this second regime is qualitatively consistent with the slow field-induced polarization of the spins that is expected in a SG. It thus appears one is dealing with a *mixed* behavior superimposing "FI" and "glassy" responses. According to our interpretation, the first feature should be associated to the polarization of ferrimagnetically coupled $(Cu^{2+})_{A'}$ and $(Mn)_B$, while the second stems from the $(Mn^{3+})_{A'}$. For $x = 2$, the subsystems $(Mn)_B$, $(Cu^{2+})_{A'}$, and $(Mn^{3+})_{A'}$ carry a magnetic moment per formula unit equal to 14, 1, and $8\mu_B$, respectively. Accordingly, the first plateau observed on the M(B) around 1 T can be regarded as the combination of a FI signal of $14-1 = 13\mu_B$, plus a partial polarization of the SG leading to $3\mu_B$. As the field is increased to larger values, this SG contribution increases up to its maximum value of $8\mu_B$, leading to $M_S = 14-1+8 = 21\mu_B$/f.u., i.e., a value compatible with that experimentally observed in Ref. 33.

The "mixed" character of the magnetic response presently observed for $x = 2$ bears a lot of similarities with the *glassy ferromagnetism* previously found in a variety of materials.[45–49] In our vision, however, we emphasize that the glassiness in $x = 2$ does not develop at a mesoscopic scale (e.g., involving magnetic domains[45] or phase separation[49]) but is rather associated to one of the elemental sublattices of the structure.

From a magnetocaloric point of view, it must be noted that normalizing M_S to the single perovskite manganite form (ABO_3) leads to values ranging from $3.7\mu_B$ for $x = 1$ to $5\mu_B$ for $x = 2$, i.e., significantly larger than the maximum $3.6\mu_B$ found in standard perovskite manganite.[39] The presence of such unusually large M_S values in oxides was precisely one of our motivations to investigate the MCE in the $Ca(Cu_{3-x}Mn_x)Mn_4O_{12}$ system.

D. Role of x in the MCE

Series of magnetic isotherms M_T(B) were recorded in the four $Ca(Cu_{3-x}Mn_x)Mn_4O_{12}$ compounds. As a representative example, the curves for $x = 1$ are shown in Fig. 8. One observes the absence of magnetic hysteresis between increasing and decreasing field, confirming that the FI-PM transition in $Ca(Cu_{3-x}Mn_x)Mn_4O_{12}$ is a SOMT. Accordingly, the isothermal entropy changes can reliably be calculated *via* the Maxwell relation,[9]

$$\Delta S_M(T,\Delta B) = S_M(T,B) - S_M(T,0) = \int_0^B \left(\frac{\partial M}{\partial T}\right)_{B'} dB'. \quad (1)$$

Figure 9 shows the obtained $-\Delta S_M$ (T) curves for the four x values and considering three values of field change: $\Delta B = 2$ T, 5 T, and 9 T. For each compound, $-\Delta S_M$ (T) exhibits a maximum around its Curie temperature. The maximum values, $-\Delta S_M^{\max}$, associated with the different field changes ($\Delta B = 2$, 5, and 9 T) are reported in Table I. Regarding applications in magnetic refrigeration, it is worth noticing that the Mn/Cu ratio allows the temperature domain of the MCE to be adjusted over a very wide range from ~30 to 320 K. A peculiar feature of these $-\Delta S_M$ (T) curves is their dissymmetrical shape, i.e., the fact that the decrease on the low-T side of the peak is considerably slower than on the high-T side. This feature becomes particularly pronounced in the $x = 2$ compound which exhibits a remarkably small slope between T_C and T_g. This kind of $-\Delta S_M$ (T) curves strongly contrasts with the roughly symmetrical behavior found in standard perovskites around their T_C.[50,51] For applications, it turns out that having a broad $-\Delta S_M$ (T) is favorable in operating modes like Active Magnetic Regeneration Refrigeration (AMRR),[52–54] which is based on the development of a temperature gradient along the active material. More precisely, the suitability of a magnetocaloric material to applications in refrigeration is often evaluated through parameters such as the RC[2–4] or the relative cooling power (RCP).[54]

The RC can be obtained by numerically integrating the area under the $-\Delta S_M$ (T) curve, using the temperatures at half maximum of the $-\Delta S_M$ peak as the integration limits:[2–4] $RC = \int_{T_1}^{T_2} \Delta S_M(T)dT$. In the literature other authors prefer using the RCP for comparison between different

TABLE I. Main magnetocaloric parameters of $Ca(Cu_{3-x}Mn_x)Mn_4O_{12}$ ($x = 1$, 1.25, 1.5, 2) compounds for different field changes.

Material x	T_{peak} (K)	$-\Delta S_M^{\max}(9T)$ (J/kg K)	$-\Delta S_M^{\max}(5T)$ (J/kg K)	$-\Delta S_M^{\max}(2T)$ (J/kg K)	$\delta T_{FWHM}(K)$ (K)	RC(2T) (J/kg)	RCP(2T) (J/kg)
1	280	5.6	3.6	1.83	78	100	143
1.25	270	5.8	3.8	1.87	92	121	172
1.5	226	5.8	3.7	1.81	146	179	264
2	163	6.6	4.0	1.9	158	223	312

TABLE II. Comparison of magnetocaloric parameters in $Ca(Cu_{3-x}Mn_x)Mn_4O_{12}$ ($x = 1, 1.25$) with some of the best single perovskite manganites and the "reference" Gd around RT.

Material	ΔB (T)	T_{peak} (K)	$-\Delta S_M^{max}$ (J/kg K)	$\delta T_{FWHM}(K)$ (K)	RC (J/kg)	RCP (J/kg)	Reference
$La_{0.7}Ca_{0.250}K_{0.050}MnO_3$	2	270	3.95	22.3	66	88	59
Gd	2	293	4.2	39.5	134	166	60
$Ca(Cu_2Mn)Mn_4O_{12}$	2	280	1.83	78	100	143	This work
$Ca(Cu_{1.75}Mn_{1.25})Mn_4O_{12}$	2	270	1.87	92	121	172	This work
$La_{0.7}Ca_{0.25}Sr_{0.05}MnO_3$	5	275	10.5	44	346	462	61
$Pr_{0.63}Sr_{0.37}MnO_3$	5	300	8.52	60	383	511	62
Gd	5	294	10.3	67	556	687	63
$Ca(Cu_2Mn)Mn_4O_{12}$	5	280	3.63	170	415	615	This work
$Ca(Cu_{1.75}Mn_{1.25})Mn_4O_{12}$	5	270	3.77	196	492	739	This work

magnetocaloric materials.[54] Considering the full width at half maximum (FWHM) ($\delta T_{FWHM} = T_2 - T_1$) and the maximum ($-\Delta S_M^{max}$), this parameter is given by $RCP = -\Delta S_M^{max} \cdot \delta T_{FWHM}$. The values of δT_{FWHM}, RC, and RCP in all the $Ca(Cu_{3-x}Mn_x)Mn_4O_{12}$ compounds are reported in Table I, considering the field change $\Delta B = 2$ T that is the most relevant to applications.

As expected owing to the shape of the $-\Delta S_M(T)$ curves, quite large values of RC and RCP are obtained. One observes in Table I that δT_{FWHM} increases with x, consistently with the fact that the substitution gives rise to an increasing magnetic inhomogeneity as discussed in previous sections. We emphasize that similar enlargements of the working temperature region induced by effects of magnetic inhomogeneity/disorder have been observed in various systems, such as bulk compounds,[3,55] nanoparticles,[56] amorphous alloys,[57] and thin films.[58]

The peak of MCE is centered close to RT for $x = 1$ and $x = 1.25$. In Table II we compared the main magnetocaloric parameters of these compounds with those of oxide and non-oxide "reference" material Gd around RT.[59–63] It is patent that the RC and RCP values of the $x = 1$ and 1.25 compounds are larger than those found in the usual perovskite manganites around RT.[51,59,61,62] For $\Delta B = 2$ T, a large δT_{FWHM} of 92 K in $x = 1.25$ compound is achieved around RT, which is more than twice as large as the value in polycrystalline Gd (≈ 40 K).[60] Thereby, although the corresponding $-\Delta S_M^{max}$ (1.87 J/kg K) is only 45% of the value in polycrystalline Gd, the RC and RCP become comparable with those of this "reference" material. Similarly, the RC or RCP values of the $x = 1.5$ compound are also larger than those of usual perovskite manganites around 226 K for the same ΔB.[51] In the case of $x = 2$, a remarkable δT_{FWHM} value of 164 K for $\Delta B = 2$ T is achieved, leading to a particularly high RC value of 223 J/kg. In Table III we compare the magnetocaloric parameters of $Ca(CuMn_2)Mn_4O_{12}$ with those of excellent perovskite oxides[64–66] and intermetallics[67–71] in the same temperature range. Clearly, the δT_{FWHM} and RC values of $Ca(CuMn_2)Mn_4O_{12}$ are much larger than in other perovskite oxides and intermetallics, suggesting it is a competitive candidate for magnetic refrigeration in this temperature range.

IV. SUMMARY

The present study allows to extend the class of RT magnetocaloric materials to the double distorted perovskites of formulation $Ca(Cu_{3-x}Mn_x)Mn_4O_{12}$. Starting from the parent compound $CaCu_3Mn_4O_{12}$ (having a FI transition at 355 K), the investigated series ($x = 1, 1.25, 1.5$, and 2) leads to compounds exhibiting a T_C spanning from RT for $x = 1$ down to $\approx$163 K for $x = 2$. For this latter value, one observes the onset of a glassy behavior below $T_g \approx 70$ K that is described as a peculiar

TABLE III. Comparison of the magnetocaloric parameters in $Ca(CuMn_2)Mn_4O_{12}$ and in representative magnetic refrigerant materials around 163 K.

Material	ΔB (T)	T_{peak} (K)	$-\Delta S_M^{max}$ (J/kg K)	$\delta T_{FWHM}(K)$ (K)	RC (J/kg)	RCP (J/kg)	Reference
$(La_{0.9}Tb_{0.1})_{2/3}Ca_{1/3}MnO_3$	1.5	166	4.76	20	72	95	64
$La_{0.80}Ca_{0.20}MnO_3$	1.5	176	3.67	30	82.5	110	65
$La_{1.6}Ca_{1.4}Mn_2O_7$	1.5	168	3.8	30	85.5	114	66
$DyCo_{1.94}Ga_{0.06}$	1.5	165	6.41	12	58	77	67
Tb_2In	1.5	165	2.6	45	88	117	68
$Ca(CuMn_2)Mn_4O_{12}$	1.5	163	1.48	138	156	204	This work
Gd_5SiGe_3	5	144	20	20	300	400	69
$GdAl_2$	5	167	7.6	88	504	669	70
$(Gd_{0.9}Dy_{0.1})_4Co_3$	5	145	8.5	66	423	560	71
$Ca(CuMn_2)Mn_4O_{12}$	5	163	4.4	186	602	751	This work

type of *glassy ferrimagnetism*. This $Ca(Cu_{3-x}Mn_x)Mn_4O_{12}$ series yields M_S values that are significantly higher than in single perovskite manganites and which increase with the Mn/Cu ratio over the investigated range. A comprehensive picture of the overall evolution of the magnetic properties as a function of x has been proposed.

As for the MCE, it turns out that the combination of large M_S with disorder-induced magnetic inhomogeneity makes these $Ca(Cu_{3-x}Mn_x)Mn_4O_{12}$ to be interesting candidates for application in a wide temperature range from 50 to 310 K. In particular, it is found that the dissymmetric $-\Delta S_M(T)$ curves of these compounds lead to RC or RCP values that are significantly larger than in usual perovskite manganites. Similarly to an increase in the x value, it also deserves to be noted that increasing the preparation temperature T_p tends to reduce T_C while increasing M_S.

In the search of large MCE around RT, it could be of great interest to investigate the likely occurrence of similar phenomena in the $LnCu_3Mn_4O_{12}$ compounds (Ln being a lanthanide[13,16] or Bi[14,72]). Indeed, as compared to $CaCu_3Mn_4O_{12}$, these materials exhibit both higher T_C (>370 K to 430 K, except 350 K in $BiCu_3Mn_4O_{12}$[72]) and larger M_S ($\geqslant 10\mu_B$/f.u., except $\sim 8\mu_B$/f.u. in $SmCu_3Mn_4O_{12}$[16]).

ACKNOWLEDGMENTS

The authors are very grateful to L. Hervé for valuable assistance in the preparation of the samples. This work has been supported by the European project "SOPRANO" under Marie Curie actions (Grant No. PITN-GA- 2008-214040) and the CNRS project "Réfrigération Magnétique" within the frame of the "Programme Interdisciplinaire Energie."

*qzhangemail@gmail.com

[1] J. Glanz, Science **279**, 2045 (1998).
[2] K. A. Gschneidner Jr., V. K. Pecharsky, A. O. Pecharsky, and C. B. Zimm, Mater. Sci. Forum. **315-317**, 69 (1999).
[3] V. Provenzano, A. J. Shapiro, and R. D. Shull, Nature (London) **429**, 853 (2004).
[4] N. S. Bingham, M. H. Phan, H. Srikanth, M. A. Torija, and C. Leighton, J. Appl. Phys. **106**, 023909 (2009).
[5] V. K. Pecharsky and K. A. Gschneidner Jr., Phys. Rev. Lett. **78**, 4494 (1997).
[6] H. Wada and Y. Tanabe, Appl. Phys. Lett. **79**, 3302 (2001).
[7] A. Fujita, S. Fujieda, Y. Hasegawa, and K. Fukamichi, Phys. Rev. B **67**, 104416 (2003).
[8] O. Tegus, E. Brück, K. H. J. Buschow, and F. R. de Boer, Nature (London) **415**, 150 (2002).
[9] E. Brück, J. Phys. D: Appl. Phys. **38**, R381 (2005); Q. Zhang, F. Guillou, A. Wahl, Y. Breard, and V. Hardy, Appl. Phys. Lett. **96**, 242506 (2010).
[10] C. M. Bonilla, J. H. Albillos, F. Bartolomé, L. M. García, and M. P. Borderías, Phys. Rev. B **81**, 224424 (2010).
[11] J. Chenavas, J. C. Joubert, M. Marezio, and B. Bochu, J. Solid State Chem. **14**, 25 (1975).
[12] B. Bochu, J. L. Buevoz, J. Chenavas, A. Collomb, J. C. Joubert, and M. Marezio, Solid State Commun. **36**, 133 (1980).
[13] A. N. Vasil'ev and O. S. Volkova, J. Low. Temp. Phys. **33**, 895 (2007).
[14] T. Saito, W. T. Chen, M. Mizumaki, J. Paul Attfield, and Y. Shimakawa, Phys. Rev. B **82**, 024426 (2010).
[15] Z. Zeng, M. Greenblatt, M. A. Subramanian, and M. Croft, Phys. Rev. Lett. **82**, 3164 (1999).
[16] J. Sánchez-Benítez, J. A. Alonso, H. Falcón, M. J. Martínez-Lope, A. de Andrés, and M. T. Fernández-Díaz, J. Phys.: Condens. Matter. **17**, S3063 (2005).
[17] R. Weht and W. E. Pickett, Phys. Rev. B **65**, 014415 (2001).
[18] I. O. Troyanchuk, L. S. Lobanovsky, N. V. Kasper, M. Hervieu, A. Maignan, C. Michel, H. Szymczak, and A. Szewczyk, Phys. Rev. B **58**, 14903 (1998).
[19] Z. Zeng, M. Greenblatt, J. E. Sunstrom, M. Croft, and S. Khalid, J Solid State Chem. **147**, 185 (1999).
[20] J. Sánchez-Benítez, C. Prieto, A. de Andrés, J. A. Alonso, M. J. Martínez-Lope, and M. T. Casais, Phys. Rev. B **70**, 024419 (2004).
[21] J. Sánchez-Benítez, J. A. Alonso, M. J. Martínez-Lope, M. T. Casais, J. L. Martínez, A. de Andrés, and M. T. Fernández-Díaz, Chem. Mater. **15**, 2193 (2003).
[22] J. Sánchez-Benitez, J. A. Alonso, A. de Andres, M. J. Martinez-Lope, M. T. Casais, and J. L. Martinez, J. Magn. Magn. Mater. **272-276**, e1407 (2004).
[23] O. Volkovaa, K. Klimov, O. Savelieva, N. Tristan, E. Goodilin, B. Buechner, and A. Vasiliev, J. Magn. Magn. Mater. **300**, e134 (2006).
[24] C. H. Chen, J. M. Gibson, and R. M. Fleming, Phys. Rev. B **26**, 184 (1982).
[25] X. Z. Yu, R. Mathieu, T. Arima, Y. Kaneko, J. P. He, M. Uchida, T. Asaka, T. Nagai, K. Kimoto, A. Asamitsu, Y. Matsui, and Y. Tokura, Phys. Rev. B **75**, 174441 (2007).
[26] Y. Zhang, H. X. Yang, Y. Q. Guo, C. Ma, H. F. Tian, J. L. Luo, and J. Q. Li, Phys. Rev. B **76**, 184105 (2007).
[27] D. M. Itkis, E. A. Goodilin, A. M. Balagurov, I. A. Bobrikov, A. S. Sinitskii, and Y. D. Tretyakov, Solid State Commun. **139**, 380 (2006).
[28] A. Prodi, G. Allodi, E. Gilioli, F. Licci, M. Marezio, F. Bolzoni, A. Gauzzi, and R. De Renzi, Physica B **374**, 55 (2006).
[29] Z. R. Yang, S. Tan, and Y. H. Zhang, Appl. Phys. Lett. **79**, 3645 (2001).
[30] A. N. Vasil'ev, O. S. Volkova, and E. A. Goodilin, JETP Letters. **101**, 367 (2005).
[31] A. J. Mydosh, *Spin Glasses: An Experimental Introduction,* (Taylor and Francis, London, 1993).
[32] Y. Bréard, V. Hardy, B. Raveau, A. Maignan, H. J. Lin, L. Y. Jang, H. H. Hsieh, and C. T. Chen, J. Phys.: Condens. Matter. **19**, 216212 (2007).
[33] O. Volkova, E. Goodilin, A. Vasiliev, D. Khomskii, N. Tristan, P. Kerschl, Y. Skourski, K. H. Mueller, and B. Buechner, JETP Letters. **82**, 642 (2005).
[34] W. Zhang, L. D. Yao, L. X. Yang, F. Y. Li, Z. X. Liu, C. Q. Jin, and R. C. Yu, J. Alloys Compd. **425**, 10 (2006).
[35] W. A. Razzaq, J. S. Kouvel, and H. Claus, Phys. Rev. B **30**, 6481, (1984).

[36]E. Moreno, V. Sagredo, and G. F. Goya, Physica B **291**, 190 (2000).
[37]R. Ranganathan, L. S. Vaidyanatban, A. Chalcravarti, and G. Rangarajan, Solid State Commun. **85**, 911 (2006).
[38]A. Collomb, D. Samaras, J. Chenavas, M. Marezio, J. C. Joubert, B. Bochu, and M. N. Deschizeaux, J. Magn. Magn. Mater. **7**, 1 (1978).
[39]J. B. Goodenough, *Magnetism and the Chemical Bond*, (Robert E. Krieger Publishing Company, Huntington, New York, 1976).
[40]H. Meskine, H. König, and S. Satpathy, Phys. Rev. B **64**, 094433 (2001).
[41]C. Zener, Phys. Rev. **82**, 403 (1951).
[42]T. Saito, W. T. Chen, M. Mizumaki, J. Paul Attfield, and Y. Shimakawa, Phys. Rev. B **82**, 024426 (2010).
[43]A. Muñoz, M. J. Martínez-Lope, M. Retuerto, H. Falcón, and J. A. Alonso, J. Appl. Phys. **104**, 083911 (2008).
[44]H. Shiraki, T. Saito, T. Yamada, M. Tsujimoto, M. Azuma, H. Kurata, S. Isoda, M. Takano, and Y. Shimakawa, Phys. Rev. B **76**, 140403(R) (2007).
[45]W. Abdul-Razzaq and J. S. Kouvel, J. Appl. Phys. **55**, 1623 (1984).
[46]D. N. H. Nam, K. Jonason, P. Nordblad, N. V. Khiem, and N. X. Phuc, Phys. Rev. B **59**, 4189 (1999).
[47]S. Mukherjee, R. Ranganathan, P. S. Anilkumar, and P. A. Joy, Phys. Rev. B **54**, 9267 (1996).
[48]K. Asai, O. Yokokura, N. Nishimori, H. Chou, J. M. Tranquada, G. Shirane, S. Higuchi, Y. Okajima, and K. Kohn, Phys. Rev. B **50**, 3025 (1994).
[49]J. Wu and C. Leighton, Phys. Rev. B **67**, 174408 (2003).
[50]Z. B. Guo, Y. W. Du, J. S. Zhu, H. Huang, W. P. Ding, and D. Feng, Phys. Rev. Lett. **78**, 1142 (1997).
[51]M. H. Phan and S. C. Yu, J. Magn. Magn. Mater. **308**, 325 (2007).
[52]B. J. Korte, V. K. Pecharsky, and K. A. Gschneidner, J. Appl. Phys. **84**, 5677 (1998).
[53]M. A. Richard, A. M. Rowe, and R. Chahine, J. Appl. Phys. **95**, 2146 (2004).
[54]K. A. Gschneidner Jr., and V. K. Pecharsky, Annu. Rev. Mater. Sci. **30**, 387 (2000).
[55]Q. Zhang, J. Du, Y. B. Li, N. K. Sun, W. B. Cui, D. Li, and Z. D. Zhang, J. Appl. Phys. **101**, 123911 (2007).
[56]P. Poddar, J. Gass, D. J. Rebar, S. Srinath, H. Srikanth, S. A. Morrisonb, and E. E. Carpenter, J. Magn. Magn. Mater. **307**, 227 (2006).
[57]Q. Y. Dong, B. G. Shen, J. Chen, J. Shen, F. Wang, H. W. Zhang, and J. R. Sun, J. Appl. Phys. **105**, 053908 (2009).
[58]Q. Zhang, S. Thota, F. Guillou, P. Padhan, V. Hardy, A. Wahl, and W. Prellier, J. Phys: Cond. Matt. **23**, 052201 (2011).
[59]M. Bejar, R. Dhahri, E. Dhahri, M. Balli, and E. K. Hlil, J. Alloys Compd. **440**, 36 (2007).
[60]N. T. Trung, Z. Q. Ou, T. J. Gortenmulder, O. Tegus, K. H. J. Buschow, and E. Brück, Appl. Phys. Lett. **94**, 102513 (2009); J. Shen, B. Gao, Q. Y. Dong, Y. X. Li, F. X. Hu, J. R. Sun, and B. G. Shen, J. Phys. D: Appl. Phys. **41**, 245005 (2008).
[61]M. H. Phan, S. C. Yu, and N. H. Hur, Appl. Phys. Lett. **86**, 072504 (2005).
[62]M. H. Phan, H. X. Peng, and S. C. Yu, J. Appl. Phys. **97**, 10M306 (2005).
[63]J. Shen, B. Gao, Q. Y. Dong, Y. X. Li, F. X. Hu, J. R. Sun, and B. G. Shen, J. Phys. D: Appl. Phys. **41**, 245005 (2008).
[64]H. Chen, C. Lin, and D. S. Dai, J. Magn. Magn. Mater. **257**, 254 (2003).
[65]M. H. Phan, V. T. Pham, S. C. Yu, J. R. Rhee, and N. H. Hur, J. Magn. Magn. Mater. **272-276**, 2337 (2004).
[66]T. J. Zhou, Z. Yu, W. Zhong, X. N. Xu, H. H. Zhang, and Y. W. Du, J. Appl. Phys. **85**, 7975 (1999).
[67]W. Q. Ao, J. Q. Li, F. S. Liu, and Y. X. Jian, Solid State Commun. **141**, 219 (2007).
[68]Q. Zhang, J. H. Cho, J. Du, F. Yang, X. G. Liu, W. J. Feng, Y. J. Zhang, J. Li, and Z. D. Zhang, Solid State Commun. **149**, 396 (2009).
[69]K. A. Gschneidner Jr., V. K. Pecharsky, A. O. Pecharsky, V. V. Ivtchenko, and E. M. Levin, J. Alloys Compd. **303-304**, 214 (2000).
[70]S. Yu. Dan'kov, V. V. Ivtchenko, A. M. Tishin, K. A. Gschneidner Jr., and V. K. Pecharsky, Adv. Cryog. Eng. **46**, 397 (2000).
[71]Q. Zhang, B. Li, X. G. Zhao, and Z. D. Zhang, J. Appl. Phys. **105**, 053902 (2009).
[72]K. Takata, I. Yamada, M. Azuma, M. Takano, and Y. Shimakawa, Phys. Rev. B **76**, 024429 (2007).